SAND2013-4405C

Continuum Simulation of Hypersonic Flows using the Quantum-Kinetic Chemical Reaction Model

Ross Wagnild* and Michael Gallis†
Engineering Sciences Center
Sandia National Laboratories
Albuquerque, New Mexico 87123

The Quantum-Kinetic (Q-K) chemical reaction model is implemented in a two-temperature Navier-Stokes solver and tested on a set high-altitude flight experiments. The chemical reaction rates predicted by the Q-K model are compared to a commonly used model for flows in thermal non-equilibrium. The results show that in thermal equilibrium the reaction rates between these two models are comparable. The Q-K predicts larger rates for some chemical reactions and smaller rates for other reactions in an five species air chemistry model. In thermal non-equilibrium, the Q-K model maintains comparable rates near thermal equilibrium, while avoiding issues of strong thermal non-equilibrium seen in the other model.

The application of the Q-K rates to the set of high-altitude flight experiments show that the Q-K model is able to remain consistent with previous Navier-Stokes and DSMC computations over altitudes ranging from $53.5\,km$ up to $87.5\,km$ despite the enforcement of translational-rotational equilibrium. The commonly used model was unable to match this performance. This work leads to further research into the performance of the Q-K model in the continuum flow regime and extending the applicability of a Navier-Stokes to higher altitudes.

I. Introduction

Although the problem of calculating chemically reacting flow fields in the rarefied hypersonic regime has been studied since the Apollo era,[1] the influence of thermal non-equilibrium on atmospheric reaction rates is still not fully understood. Multiple theoretical and empirical methods have been proposed that aim to capture the impact of non-equilibrium energy distribution between the available energy modes on chemical reaction rates.[2] A common issue with these models is that they rely on experimental data taken at conditions that do not match the flight environment and therefore employ empirical fits extrapolated to flight conditions.

Bird proposed[3] new types of chemical reaction models, termed the Quantum-Kinetic (Q-K) model,[4] based solely on properties of the colliding molecules, that do not use measured equilibrium reaction rates or any adjustable parameters. The microscopic properties used in these models include the available collision energy, dissociation energies, and quantized vibrational energy levels. These chemical reaction models link the chemical-reaction process to the energy content of the vibrational modes of the colliding molecules. Application of chemical-reaction procedures for collisions between molecules that could lead to endothermic reactions is conceptually straightforward. The models for these "forward" endothermic reactions and the principle of microscopic reversibility are then used to develop models for the corresponding "reverse" exothermic reactions. These models satisfy microscopic reversibility by balancing the fluxes into and out of each state and do not require any macroscopic rate information.

The lack of adjustable parameters means that these models cannot be calibrated to reproduce a given equilibrium reaction rate. Instead, the new models predict reaction rates, even for thermal non-equilibrium

*Senior Member of Technical Staff, Member AIAA
†Principal Member of Technical Staff, Senior Member AIAA

conditions. For dissociation, ionization, and exchange reaction types, the models produce equilibrium reaction rates that are in good qualitative and quantitative agreement with the best available theoretical and measured or extrapolated reaction rates.[5] The differences between the most reliable reaction rates and the corresponding Q-K values are usually less than an order of magnitude, which typically is comparable to the uncertainties in measurements.

Besides their conceptual simplicity and their apparent ability to reproduce known rates, a significant advantage of these models is that, although originally proposed for use in DSMC codes, the Q-K model, allows the derivation of closed-form solutions for the reaction rates. Thus, these rates, and in particular, the non-equilibrium ones can be used within the context of the Navier-Stokes equations.

Currently, the ability to simulate upper-atmosphere hypersonic flows and environments is hampered by using chemical-reaction-rate models of unknown accuracy that introduce unknown errors into calculations. The Q-K models have the potential to lead to a predictive and self-consistent capability for determining equilibrium and non-equilibrium chemical-reaction rates that do not rely on measured equilibrium rates. These models also simplify validation and uncertainty quantification relative to empirical models because they use no adjustable macroscopic parameters.

In the current study, these first-principle models are applied in a two-temperature Navier-Stokes solver, US3D.[9] The chemical reaction rates are first compared to a reaction model commonly used in reacting flows involving thermal non-equilibrium based on data from Park[16] and Park et al.[17] Next, the Q-K models are applied to a high-altitude flight experiment. The results of these computations are compared to previous calculations in order to gauge the ability of the Q-K models to predict accurate flow compositions at different altitudes.

II. Mathematical Model

II.A. Dissociation Reaction Rate

The general reaction rate defined by Gallis et al.[6] is as follows

$$k_{diss}\left(T,T_v\right)=\frac{2\sigma_{ref}}{\varepsilon\sqrt{\pi}}\left(\frac{T}{T_{ref}}\right)^{1-\omega}\left(\frac{2k_BT_{ref}}{m_r}\right)^{1/2}\left[\Phi_{vib}\left(T,T_v\right)+B\Psi_{vib}\left(T_v\right)\right], \tag{1}$$

where σ_{ref} is the collision cross section at the reference temperature T_{ref}, ω is the viscosity temperature exponent, m_r is the reduced mass of the colliding pair of molecules, k_B is Boltzmann's constant, B is the truncation parameter, and ε is the symmetry parameter. The collision cross section has the form

$$\sigma_{ref}=\pi\frac{\left(d_1+d_2\right)^2}{4},$$

where $d_{(s)}$ is the molecular diameter of collision partner s at the reference temperature. The value of ω used is the simple average of the two molecules colliding. The truncation parameter takes a value of either 0 or 1. A value of zero implies that the molecular vibration model is limited to energies below the dissociation energy, while a value of 1 allows for the entire set of energy levels for the molecular vibration model. For the current work, we use the simple harmonic oscillator model for the molecular vibration model. The symmetry parameter takes a value of 1 for similar molecules and a value of 2 for dissimilar molecules. The functions Φ_{vib} and Ψ_{vib} contain the contribution of the energy due to the vibration levels of the molecule dissociating. The Φ_{vib} function is evaluated as follows

$$\Phi_{vib}=\frac{1}{z_{vib}(T_v)}\sum_{i=0}^{i_d}Q\left[\frac{5}{2}-\omega,\frac{\theta_d-i\theta_v}{T}\right]\exp\left(-\frac{i\theta_v}{T_v}\right) \tag{2}$$

where $z_{vib}(T)$ is the vibrational partition function and is equal to

$$z_{vib}(T_v)=\left(1-\exp\left(-\frac{\theta_v}{T_v}\right)\right)^{-1}.$$

The variable θ_d is the characteristic temperature of the dissociation reaction and θ_v is the characteristic vibrational temperature. The function Q is the probability of the collisional translation energy of the

molecules exceeding the difference between the vibrational level i and the dissociation level, $i_d = \text{floor}\left(\theta_d/\theta_v\right)$. This probability is evaluated as

$$Q\left(a,x\right) = \frac{\Gamma\left(a,x\right)}{\Gamma\left(a\right)},$$

where $\Gamma\left(a,x\right)$ is the upper incomplete gamma function and $\Gamma\left(a\right)$ is the complete gamma function. The complete gamma, upper incomplete gamma, and lower incomplete gamma functions are written mathetically as

$$\Gamma\left(a\right) = \int_0^\infty e^{-t}t^{a-1}dt,$$

$$\Gamma\left(a,x\right) = \int_x^\infty e^{-t}t^{a-1}dt,$$

$$\gamma\left(a,x\right) = \int_0^x e^{-t}t^{a-1}dt,$$

respectively, and can be solved for numerically using methods from Numerical Recipes. The Ψ function is as follows

$$\Psi_{vib} = \frac{1}{z_{vib}(T_v)} \sum_{i=i_d+1}^{\infty} \exp\left(-\frac{i\theta_v}{T_v}\right).$$

For the current work, we will assume that the vibrational energy levels above the dissociation level are inaccessible, or $B = 0$.

II.B. Endothermic Exchange Reaction Rate

Gallis et al.[7] define the endothermic exchange reaction rate in thermal equilibrium as

$$k_{exch}\left(T\right) = \frac{2\sigma_{ref}}{\varepsilon\sqrt{\pi}}\left(\frac{T}{T_{ref}}\right)^{1-\omega}\left(\frac{2k_BT_{ref}}{m_r}\right)^{1/2}\left(\exp\left(-\frac{C_1}{T}\right) - \exp\left(-\frac{C_2}{T}\right)\right). \tag{3}$$

The constants, C_1 and C_2 are left as constants because of the variability in the interpretation of the QK model. If one chooses to maintain the discretized nature of the DSMC model, then the constants are defined as

$$C_1 = i_a\theta_v \ ; \ i_a = \text{floor}\left(\frac{\theta_r}{\theta_v}\right) + 1,$$

$$C_2 = i_d\theta_v \ ; \ i_d = \text{floor}\left(\frac{\theta_d}{\theta_v}\right),$$

where i_a is the first vibrational level above the energy threshold of the reaction, θ_r is the characteristic temperature of the exchange reaction, i_d is the vibrational level at dissociation of the reaction partner with the lowest characteristic dissociation temperature, θ_d. The other interpretation of the QK model follows Bird's method[8] and enforces continuity of the chemical reaction rate coefficients, which is defined as

$$C_1 = \theta_r + \theta_v,$$

$$C_2 = \theta_d.$$

In the current study, we maintain the discretized nature of the DSMC model.

In order to incorporate some effect of translational-vibrational non-equilibrium, a modification of Eq. 3 is needed. It is assumed that the collision frequency of the molecules only depends on the translational temperature, therefore the collision frequency portion of the rate remains unchanged. The exponents are essentially a ratio of the energy required to cause a reaction to an energy contained within colliding molecules. To account for translational-vibrational non-equilibrium in the energy contained within colliding molecules,

an average temperature is used in the evaluation of the exponents. For the current implementation, this average temperature is calculated as

$$T_{av}\left(T,T_v\right)=\frac{(3+2)T+2T_v}{(3+2)+2},$$

where the translational-rotational contribution is given as $3+2$ to signify the three degrees of translational freedom and the two degrees of the rotational freedom of a linear molecule. Although the energy contained with a vibrational mode is not always equivalent to 2 degrees of translation motion, it serves a means of approximating the effect of thermal non-equilibrium. Therefore, the rate equation looks as follows

$$k_{exch}\left(T,T_v\right)=\frac{2\sigma_{ref}}{\varepsilon\sqrt{\pi}}\left(\frac{T}{T_{ref}}\right)^{1-\omega}\left(\frac{2k_BT_{ref}}{m_r}\right)^{1/2}\left(\exp\left(-\frac{C_1}{T_{av}\left(T,T_v\right)}\right)-\exp\left(-\frac{C_2}{T_{av}\left(T,T_v\right)}\right)\right).$$

III. Computational Method

III.A. Navier-Stokes Simulation Method

We solve the reacting, three-dimensional Navier-Stokes equations with a modified version of the unstructured CFD solver US3D.[9] This code uses the finite volume formulation and has several different inviscid flux schemes, shock detection methods, and time integration methods. For the current study, the inviscid fluxes are calculated using the Modified Steger-Warming method. Second-order spatial accuracy is accomplished with a MUSCL limiter as the TVD scheme. The viscous fluxes are evaluated using gradient reconstruction calculated using the weighted, least-squares method. The time advancement method used is the first-order implicit DPLR.[10]

The gas is simulated using a five species model composed of N_2, O_2, NO, N, and O. The viscosity for each species is calculated using a Blottner model and translational thermal conductivities are calculated using the Eucken relation. Mixture properties are calculated with Wilke's semi-empirical mixing law.

A two temperature model is used in which the molecular translational and rotational motion are described by the translational temperature, T, and the molecular vibration is described by vibrational temperature, T_v. The translational-vibrational energy exchanges are governed by the Laudau-Teller model for the simple harmonic oscillator. The characteristic relaxation times are based on the Millikan and White model.[11] It is assumed that the vibration-vibration energy exchanges are sufficiently fast to allow for a single vibrational temperature to describe the vibrational state of the gas mixture. This is a limitation of the current Navier-Stokes method. As evident in previous studies,[12–15] one key feature of high-altitude hypersonic flow is non-equilibrium between the various vibrational modes of the gas in addition to the translational-rotational-vibrational thermal non-equilibrium. In future works, a more detailed internal energy model will be implemented.

To simulate finite-rate chemistry, three models are implemented to compute a five reaction set, given in Eqns 4. The first model is the based Park[16] and Park et al.[17] The forward rates are calculated with the modified Arrhenius equation. The dissociation reactions are governed by the geometric mean of the translational and vibrational temperatures to account vibration-dissociation coupling, the TTv model, given in general form by

$$T_{eff}=T^qT^{1-q}.$$

For the current work, q is set to 0.5. The exchange reactions are governed only by the translational temperature. The backward rates for both types of reactions are governed by the translational temperature and are calculated from the forward rate and the equilibrium constant defined in Park.[16] The second model uses the Q-K approach described above to compute the reaction rates of each dissociation reaction, while maintaining the Park model for the exchange rates. Finally, the third model uses the Q-K approach to compute the reaction rates of both the dissociation reactions and the exchange reactions. In the following paragraphs, each chemistry model will be referred to by the method used to calculate the dissociation reaction rate and the exchange reaction rate. All backward rates in Q-K models depend on the forward rate and the equilibrium constant defined in Park.[16]

$$
\begin{aligned}
N_2 + M &\leftrightarrow 2N + M \\
O_2 + M &\leftrightarrow 2O + M \\
NO + M &\leftrightarrow N + O + M \\
NO + O &\leftrightarrow O_2 + N \\
N_2 + O &\leftrightarrow NO + N
\end{aligned}
\tag{4}
$$

III.B. DSMC Simulation Method

The particular DSMC method used in this study is that of Bird.[4] The massively parallel processor implementation, Icarus, is described by Bartel et al.[18] In brief, the DSMC method is applied as follows. The computational domain is populated with "computational molecules", each of which typically represents a large number of identical real molecules or atoms. During one time step, computational molecules move from one location to another, interact with boundaries, experience collisions, and are sampled to accumulate statistics. During a move, computational molecules travel at constant velocity for the entire time step or until a boundary is encountered. In the latter situation, the appropriate boundary condition is applied and the remaining portion of the time step is completed. Typical boundary conditions are "inflow" (computational molecules enter the domain with a prescribed Maxwellian distribution), "outflow" (computational molecules crossing this boundary are deleted, appropriate for supersonic applications), "diffuse wall" (computational molecules are reflected with a prescribed Maxwellian distribution), and "specular wall" (computational molecules are reflected with mirror symmetry).

Following movement and boundary interactions, computational molecules experience "collisions," which change their velocities. It should be noted that computational molecules have three-dimensional velocity vectors for collision purposes even if a two-dimensional geometry is considered. After the collision phase, statistics (e.g., number density, velocity, and temperature) are accumulated on the computational mesh, which exists only for this purpose and for determining possible collision pairs. To preclude non-physical behavior, the mesh cell spacing is constrained to be less than one-third of a local mean free path and the characteristic length scale based on local flow gradients, and the time step is similarly constrained to less than a mean collision time.

The Icarus DSMC code was written for massively parallel computing environments to allow for the large computational requirements of the DSMC method for near-continuum flows.

III.C. BSUV Flight Conditions and Geometry

In the current study, the Bow Shock UltraViolet (BSUV) experiments[19,20] are used to serve as relevant test cases for high altitude, non-equilibrium flow. These experiments measured the ultraviolet emission from the bow shock and shock layer along the stagnation streamline of a blunt-nosed cone with a radius of $0.1016\,cm$ ($4\,inches$). One of the primary radiators in the ultraviolet range from the flowfield is NO. Thus, the experiment effectively measured the concentration and temperatures of NO in the flowfield. Since NO is the result of thermal and chemical non-equilibrium of air, these experiments allow for validation of the non-equilibrium aspects of the chemistry model applied in the simulation. In addition to the experimental data available, several previous studies[13–15,21–24] have analyzed the flight data. These studies provide additional data to which results comparison can be made.

The first flight[19] flew at a velocity of approximately $3.5\,km/s$ between the altitudes of 37 and $75\,km$. The second flight[20] flew at a velocity of approximately $5.1\,km/s$ between the altitudes of 65 and $90\,km$. The first test case is from flight 1 at an altitude of $53.5\,km$, with freestream conditions contained in Table 1. The next three test cases are from flight 2 at altitudes of $79\,km$, $85\,km$, $87.5\,km$, with freestream conditions contained in Tables 2, 3, and 4, respectively. Because of the location of the instrumentation on the vehicle and the important role NO played in the measured spectra, we are primarily interested in the NO concentrations along the stagnation streamline. Therefore, we simulate only the nose of the each vehicle on an axi-symmetric, shock-tailored grid. For the continuum calculations, a "no-slip" wall boundary condition is enforced on the vehicle surface with a constant wall temperature of $500\,K$. For the DSMC simulations, the diffuse wall condition is applied such that the molecules reflecting off of the wall have a translational temperature of $500\,K$.

Table 1: Freestream Conditions for Test Case 1.

Density (kg/m^3)	$6.42 \cdot 10^{-4}$
Velocity (m/s)	3500
Temperature (K)	263.65
Mass Fraction N_2	0.7663
Mass Fraction O_2	0.2337

Table 2: Freestream Conditions for Test Case 2.

Density (kg/m^3)	$1.85 \cdot 10^{-5}$
Velocity (m/s)	5100
Temperature (K)	198.65
Mass Fraction N_2	0.7663
Mass Fraction O_2	0.2337

Table 3: Freestream Conditions for Test Case 3.

Density (kg/m^3)	$6.77 \cdot 10^{-6}$
Velocity (m/s)	5100
Temperature (K)	186.95
Mass Fraction N_2	0.7663
Mass Fraction O_2	0.2337

Table 4: Freestream Conditions for Test Case 4.

Density (kg/m^3)	$5.33 \cdot 10^{-6}$
Velocity (m/s)	5100
Temperature (K)	186.87
Mass Fraction N_2	0.7663
Mass Fraction O_2	0.2337

IV. Reaction Rate Comparisons

In previous studies,[5–8] the Q-K model has been compared to numerous theoretical and experimentally measured reaction rates for molecules in both thermal equilibrium and non-equilibrium. Although differences exist, the Q-K model has generally been within the bounds of uncertainty when compared to other theoretical, non-equilibrium reaction rate models. Since the focus of the current work is in comparing a standard Park chemistry model to that of the Q-K model, a comparison between only these models is presented in this paper.

IV.A. Thermal Equilibrium Reaction Rates

For each dissociation reaction included in Eqs. 4, a reaction rate due to a collision with a diatomic species and an atomic species is calculated from each model and compared in Figure 1 below and Figure 11 in the appendix. The Q-K model predicts dissociation reaction rates higher than the Park model for some reactions, an example is given in Figure 1a, while predicting lower rates for other reactions, an example is given in Figure 1b. With the exception of the NO dissociation reaction rates, the Q-K model predicts dissociation reaction rates within an order of magnitude for the temperature range tested. As stated by Gallis et al.,[5] the uncertainty is greater for the NO dissociation due to the competing exchange reactions. Therefore, it is expected that a greater difference between the predicted rates could exist.

For both of the exchange reactions in Eqs. 4, the Q-K model reaction rates are generally greater than or nearly equal to the Park model rates. This same trend was shown in the previous study by Gallis et al.,[6] as well.

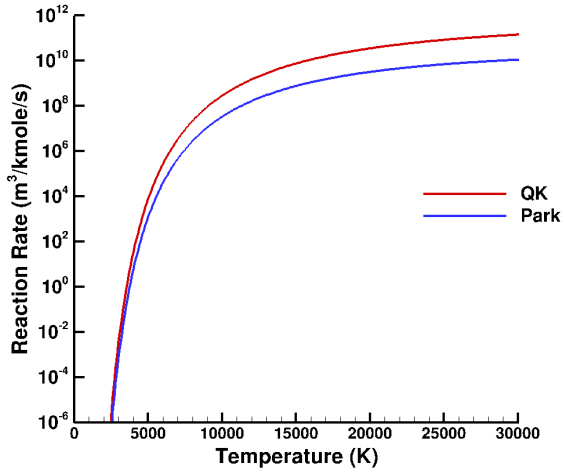

(a) $N_2 + N_2 \rightarrow 2N + N_2$

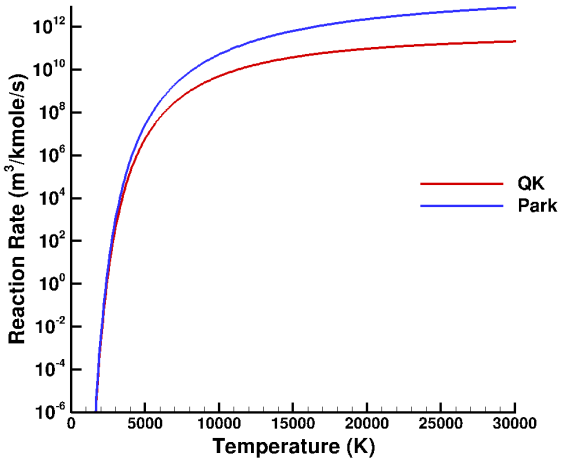

(b) $NO + NO \rightarrow N + O + NO$

Figure 1: Comparisons of select dissociation reaction rates versus temperature between the Park and Q-K models in thermal equilibrium.

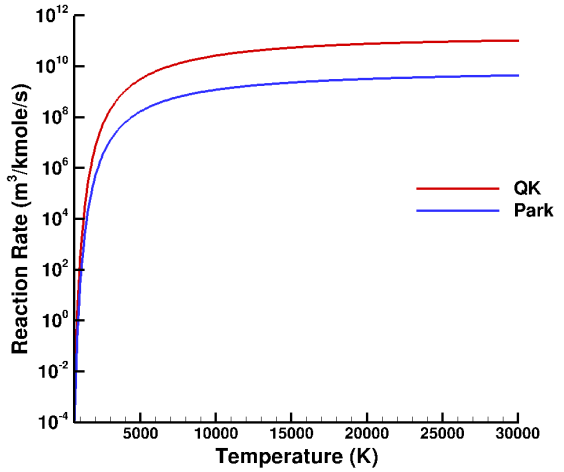

(a) $NO + O \rightarrow O_2 + N$

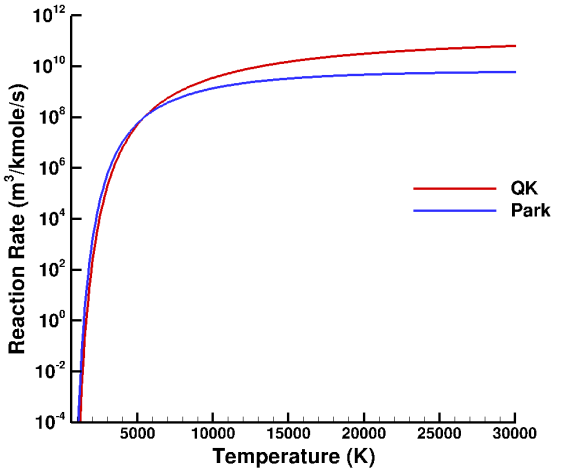

(b) $N_2 + O \rightarrow NO + N$

Figure 2: Comparisons of select endothermic exchange reaction rates versus temperature between the Park and Q-K models in thermal equilibrium.

IV.B. Thermal Non-Equilibrium Reaction Rates

The same dissociation reactions used in the thermal equilibrium comparisons are used to compare dissociation reaction rates in thermal non-equilibrium and are given in Figure 3 below and Figure 12 in the appendix. As seen in all sample reaction rates, the well known issue with the TTV model results in a reaction rate that limits to zero as the vibrational temperature approaches zero regardless of the translational temperature. The Q-K model avoids this issue because the Φ_{vib} function, given in Eq. 2, becomes

$$\Phi_{vib} = Q\left[\frac{5}{2} - \omega, \frac{\theta_d}{T}\right].$$

This property allows the Q-K model to predict chemical reactions purely from the collisional energy between molecules. Therefore, the Q-K model generally predicts higher reaction rates of dissociation for vibrational temperatures lower than the translational temperature. For vibrational temperatures higher than the translational temperature, the Q-K model predicts higher reaction rates than the Park model for some dissociation reactions, an example is given in Figure 3a, while it predicts lower reaction rates for others, an example is given in Figure 3b.

For the exchange reaction rates, the Park model does not include any translational-vibrational coupling. Therefore the reaction rates remain constant when varying the vibrational temperature and holding the translational temperature fixed, as seen in Figures 4a and 4b. The effect of the average temperature used in the Q-K exchange reactions is as expected: the predicted reaction rate decreases with a decreasing vibrational temperature and increases with an increasing vibrational temperature relative to the equilibrium rates. The result of this behavior causes the $N_2 + O \rightarrow NO + N$ reaction rate predicted by the Q-K model to be lower than the Park model over a small range of vibrational temperatures. In the case of the $NO + O \rightarrow O_2 + N$ reaction, the predicted Q-K rates remain larger than the Park model for the temperature ranges tested.

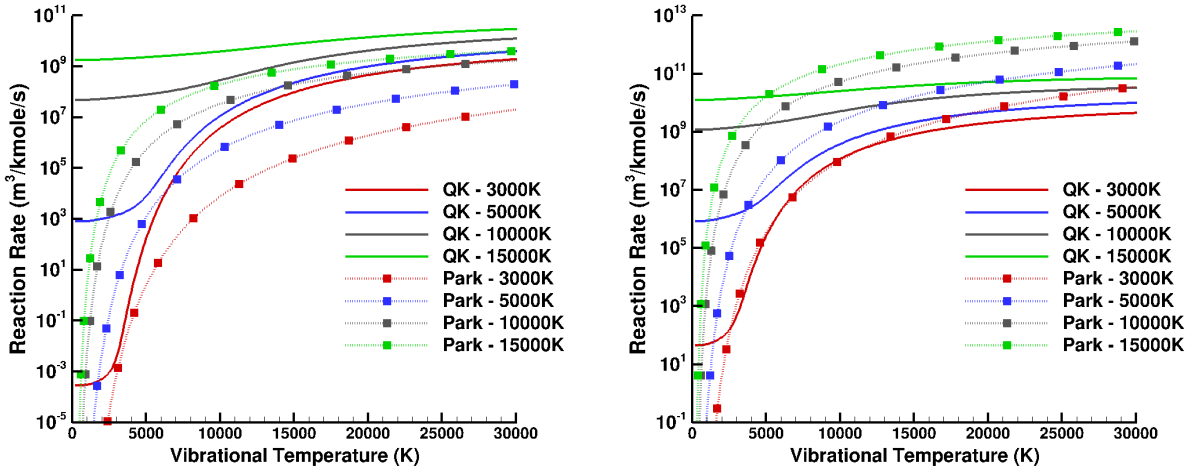

(a) $N_2 + N_2 \rightarrow 2N + N_2$ (b) $NO + NO \rightarrow N + O + NO$

Figure 3: Comparisons of select dissociation reaction rates versus vibrational temperature between the Park and Q-K models in thermal non-equilibrium.

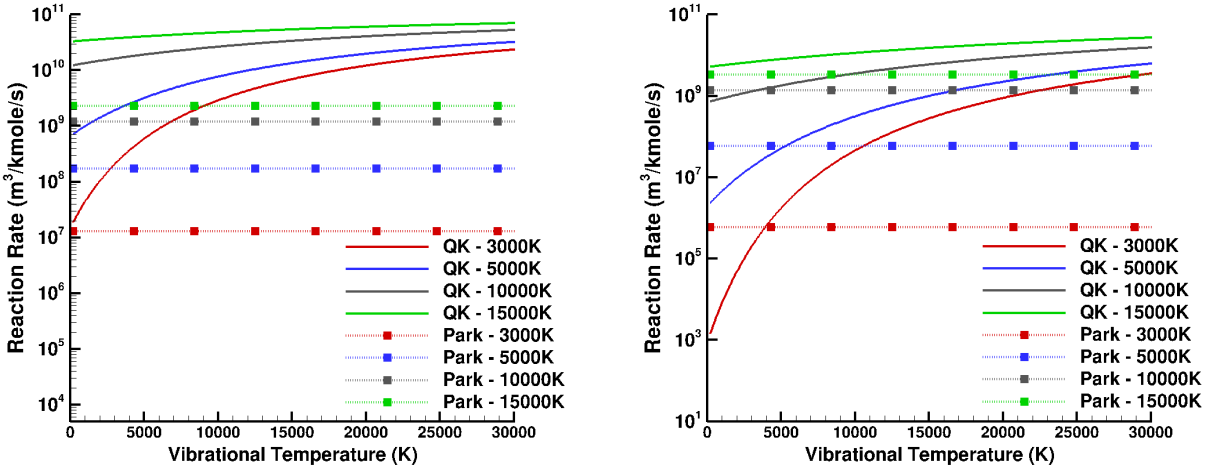

(a) $NO + O \rightarrow O_2 + N$ (b) $N_2 + O \rightarrow NO + N$

Figure 4: Comparisons of select endothermic exchange reaction rates versus vibrational temperature between the Park and Q-K models in thermal non-equilibrium.

V. BSUV Simulation Results

As stated above, the primary interest in the simulated flowfields is the NO concentration along the stagnation streamline due to its importance in the radiation spectra measured during the flights. A comparison of the NO mass fraction between the three different chemistry models from the $53.5\,km$ case, seen in Fig. 5a, shows that the Park-Park model produces the least amount of NO. The reason for this lies in the known deficiency of the TTv model in the presence of strong non-equilibrium discussed above. The translational and vibrational temperatures downstream of the shock, shown in Fig. 5b, differ by an order of magnitude, implying that the assumption of near thermal equilibrium is no longer applicable. The result of the TTv model behavior is that the production of NO does not begin until well into the shock layer, where the translation and vibrational temperatures are nearing equilibrium. Both chemistry models using Q-K for the dissociation reaction rates begin generating the species required to produce NO shortly after the shock in the presence of strong thermal non-equilibrium. As described above, the Q-K model captures the ability of molecules to dissociate at low vibrational energies given a sufficient translational energy. The Q-K-Park model produces the largest amount of NO due to this model having larger exchange reaction rates in the calculated temperature range.

A comparison of the Park-Park model of the current paper to the baseline model of Bose[13] and Bose and Candler,[12] also in Fig. 5a, shows that these two models predict similar mass fractions of NO due to the similarities between the models. The mean translational and vibrational temperatures of the gas and the shock stand-off distance are very similar. The more detailed chemistry models predict a different trend in the mass fraction of NO. The Q-K models (Q-K-Park and Q-K-Q-K) predict a greater mass fraction of NO, while the most detailed models used by Bose (models 2 and 3) predict a lower mass fraction of NO compared to the baseline models. The Q-K-Q-K model predicts very similar peaks in the translational and vibrational temperatures compared with data from Bose,[13] seen in Fig. 5b, although the shock stand-off distance and distribution of tranlational and vibrational energies through the shock layer are different.

A comparison of the NO particle density, seen in Fig. 6, shows that the Q-K models predict greater particle densities than similar altitudes computed in Levin et al.[24] The model used in Levin et al.[24] includes a separate rotational temperature relaxation process and altered vibrational relaxation parameters.

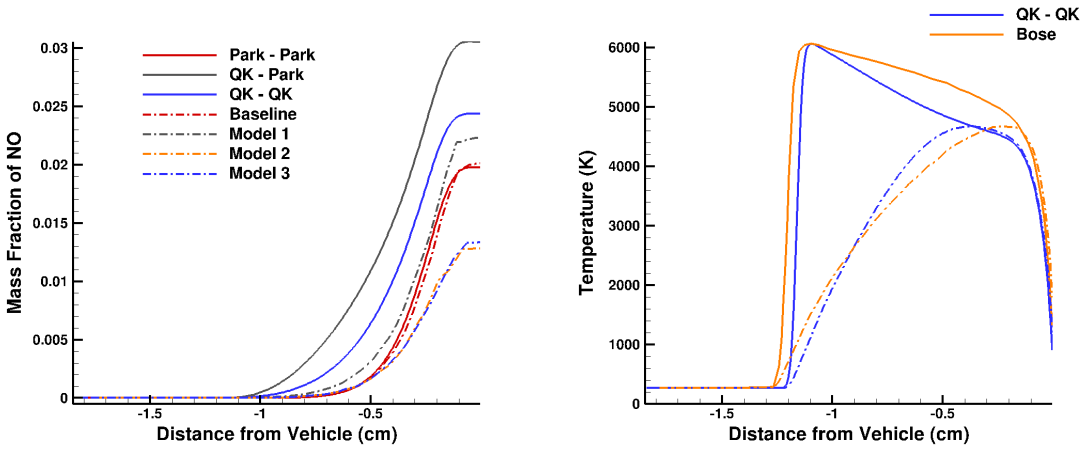

(a) Mass fraction of NO (b) Temperatures (solid - T, dash-dot - Tv)

Figure 5: Mass fraction of NO and temperatures versus distance from the vehicle along the stagnation line at an altitude of $53.5\,km$. Comparison data is from Bose.[13]

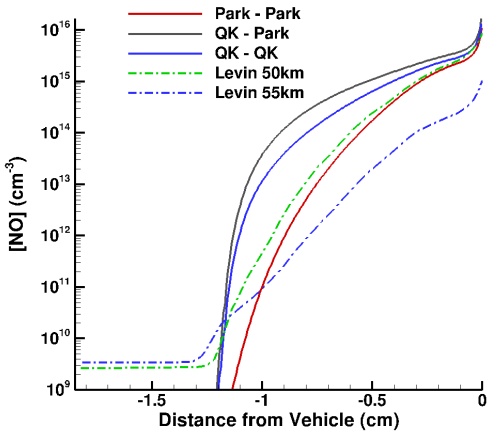

Figure 6: Predicted particle density of NO versus distance from the vehicle along the stagnation line at an altitude of $53.5\,km$. Comparison data is from Levin et al.[24] and is calculated at the altitude given in the plot legend.

In Case 2 at $79\,km$, the Park-Park model predicts a mass fraction that is two orders of magnitude less than the other two chemistry models of the current paper, shown in Fig. 7a. At this altitude and velocity, the translational and vibrational temperatures remain in strong thermal non-equilibrium until very near the wall, shown in Fig. 7b. The strong non-equilibrium is due to the diminished transfer of energy between the translational motion and vibration motion of the molecules. As a result, the geometric mean of temperatures does not reach the levels required for significant dissociation of O_2. Due to the total collision energy basis of the Q-K model, the two chemistry models using the Q-K dissociation rates predict O_2 dissociation shortly after the beginning of the bow shock. In this case, the Q-K-Q-K chemistry model predicts a greater mass fraction of NO than the Q-K-Park model because the Q-K-Q-K model predicts a higher reaction rate for $O_2 + N \rightarrow NO + O$ reaction in this temperature range.

The models used in Bose[13] and Bose and Candler[12] predict mass fractions of NO that lie within a factor of two of each other and an order of magnitude less than the Q-K models, seen in Fig. 7a. Bose's models begin producing NO earlier than the current models due to the shock stand-off distance being greater.

The NO particle density, seen in Fig. 8a, shows the same two-orders-of-magnitude difference between the Park-Park model and the Q-K models as seen in Fig. 7a. Comparing the current models to two DSMC

methods, one described above and the other used by Boyd et al.,[14] shows that the current models bracket the DSMC results by approximately an order of magnitude through the shock layer. Near the vehicle wall the Icarus data approach the Park-Park model particle density and differ at the wall by approximately a factor of two.

The translational temperature along the stagnation streamline vary widely across the various models considered, shown in Fig. 8b. The Park-Park model has a higher shock layer temperature and a larger shock stand-off distance compared to the Q-K models, resulting in a more similar location for the initiation of NO production as compared to the $53.5\,km$ case, shown in Fig. 5a. The other models all show higher translation temperatures and larger shock stand-off distances. This is largely due to the other models allowing for translational-rotational non-equilbrium. As described in several studies,[13–15] the BSUV 2 flowfields contain a large degree of translational-rotational non-equilbirium. The enforcement of thermal equilibrium between the translational and rotational motions limits the translational temperature in the current models. The effect of this limitation in model has yet to be tested. The Icarus calculation predicts the largest shock stand-off distance and begins producing NO well before the other models considered.

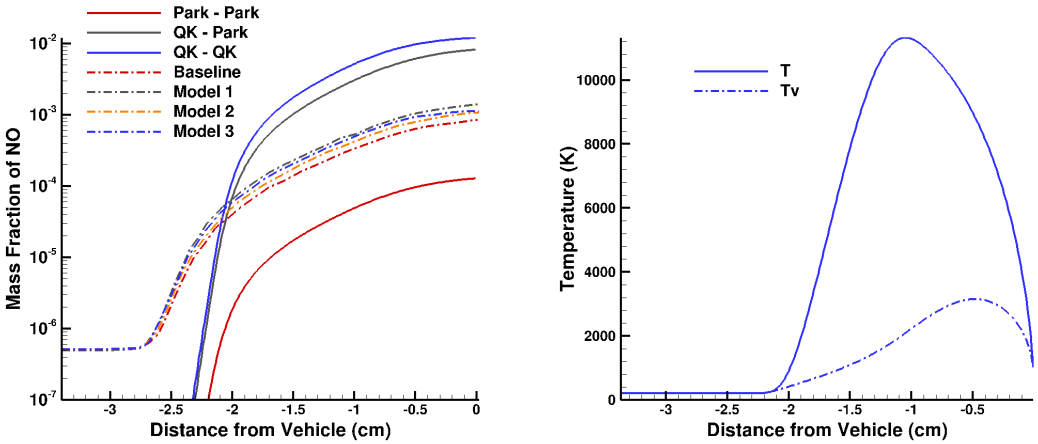

(a) Mass fraction of NO

(b) Temperatures

Figure 7: Mass fraction of NO and temperatures versus distance from the vehicle along the stagnation line at an altitude of $79\,km$. Comparison data is from Bose.[13]

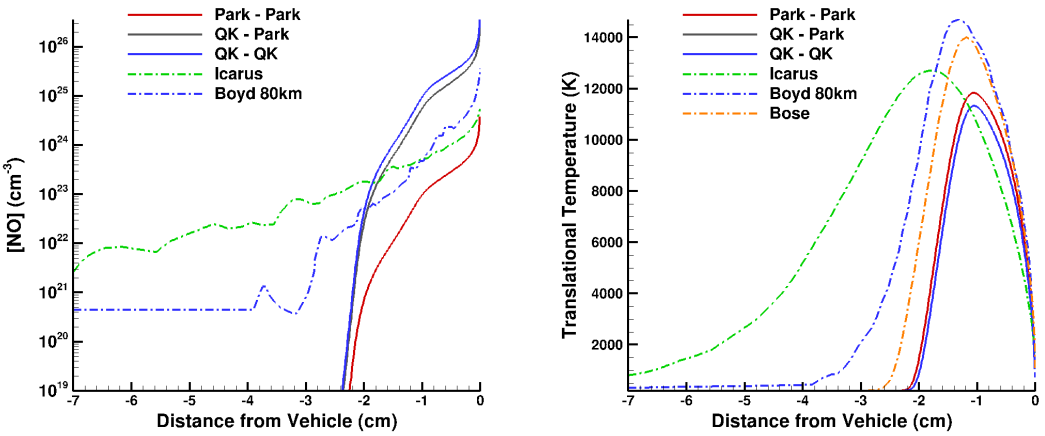

(a) Particle density of NO (b) Tranlational temperature

Figure 8: Predicted particle density of NO and translation temperature versus distance from the vehicle along the stagnation line at an altitude of $79\,km$ (Boyd data is calculated at $80\,km$). Comparison data is from Boyd et al.[14] and Bose.[13]

In the $85\,km$ case, the Park-Park model predicts a mass fraction of NO that is five orders of magnitude less than the Q-K models, while the Q-K models are within approximately ten percent of each other in the shock layer, shown in Fig. 9a. The Q-K-Q-K model predicts the largest mass fraction of NO due to the higher reaction rates for $O_2+N \rightarrow NO+O$ reaction as in the previous case. Comparing to the mass fractions of Bose,[13] the Q-K-Q-K model predicts a mass fraction that is approximately an order of magnitude greater that Bose's model 1. Comparing to the DSMC results of Icarus, shown in Fig. 9b, the particle density of the Q-K models lie approximately two orders of magnitude below Icarus immediately downstream of the shock. The Q-K models predict a larger production of NO throughout the shock layer, allowing for the Q-K models and the Icarus calculation to predict approximately the same particle density of NO at the vehicle surface despite the Icarus shock stand-off distance being twice that of the current models.

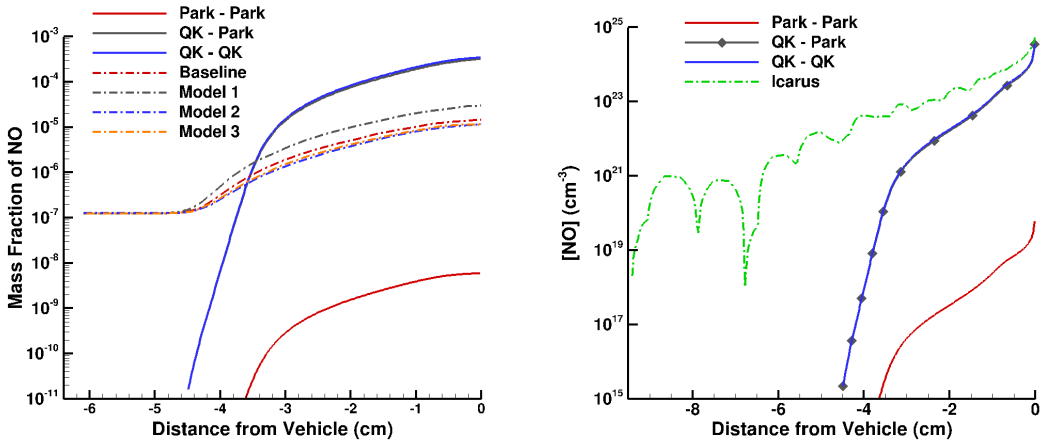

(a) Mass fraction of NO (b) Particle density of NO

Figure 9: Mass fraction and particle density of NO versus distance from the vehicle along the stagnation line at an altitude of $85\,km$. Comparison data is from Bose.[13]

In the highest altitude case tested, $87.5\,km$, the Park-Park model predicts 5.5 orders of magnitude fewer particles than the Q-K models, shown in Fig. 10a. The DSMC calculations of Icarus and from Boyd et al.[14] differ by a factor of approximately thirty, despite have similar translational temperatures and shock stand-off

distances, shown in Fig. 10b. As in the previous case, the Q-K models predict a similar particle density of NO at the vehicle surface as the Icarus prediction. The Q-K models are bounded from above by the Icarus data and from below by data from Boyd et al.[14] in the shock layer.

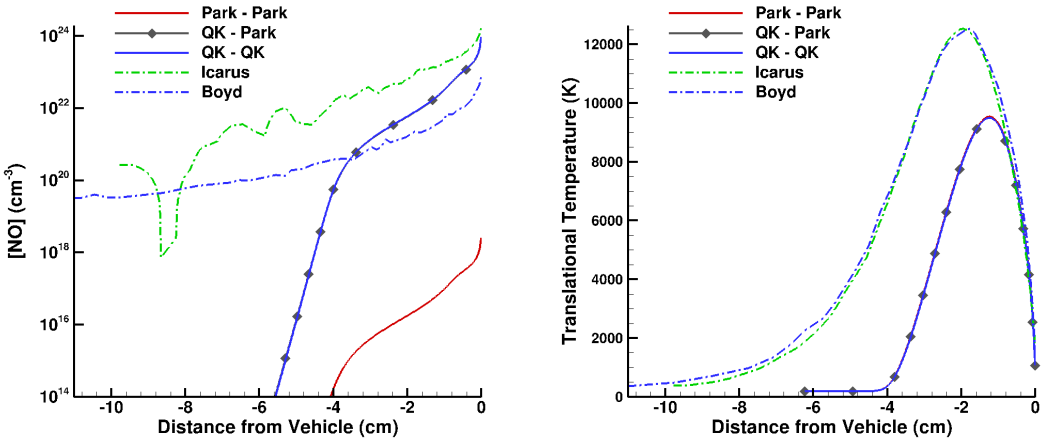

(a) Particle density of NO (b) Translational temperature

Figure 10: Particle density of NO and translational temperature versus distance from the vehicle along the stagnation line at an altitude of 87.5 km. Comparison data is from Boyd et al.[14]

VI. Summary and Conclusions

The Q-K model proposed by Bird[3,4] has been implemented in a two-temperature Navier-Stokes solver, US3D, and tested on the high-altitude flight experiments, BSUV 1[19] and 2.[20] A comparison to a commonly used Park[16,17] model showed that in the presence of thermal equilibrium the Q-K model predicts larger dissociation reaction rates for some reactions ($O_2 + O_2$ and $N_2 + N_2$) while it predicts smaller dissociation reaction rates for others ($O_2 + O$ and $NO + NO$). For endothermic exchange reactions, the Q-K model generally predicts larger forwar reaction rates.

In thermal non-equilibrium, the Q-K model maintains an increasing dissociation reaction rate with increasing vibrational temperatures. The Q-K model also avoids the low reaction rates caused by low vibrational temperature, which is a well known issue with the TTV model commonly used for thermal non-equilibrium flows. For the exchange reactions, the Q-K model continues to increase from its thermal equilibrium value with increasing vibrational temperatures. At lower vibrational temperatures, the reaction rates become comparable to or smaller than the rates in the Park model due to the Park model's lack of dependence on the vibrational energy.

For the computations of the BSUV flight experiments, the Navier-Stokes solver, US3D, was able to maintain mass fractions and particle densities generally consistent with previous Navier-Stokes simulations as well as previous and current DSMC calculations over altitudes ranging from 53.5 km up to 87.5 km. The commonly used Park model was unable to match this performance. One flaw with the current implementation is the enforcement of translational-rotational equilibrium. Additionally, the current implementation also lacks the detailed energy modeling described by Bose[13] and Bose and Candler.[12] The effects of these issues have yet to be tested. Future implementations of the Q-K model in a Navier-Stokes solver will address these issues.

VII. Acknowledgements

The authors would like to thank Dr. Graham Candler for the use of US3D. Sandia National Laboratories is a multi-program laboratory managed and operated by Sandia Corporation, a wholly owned subsidiary of Lockheed Martin Corporation, for the U.S. Department of Energy's National Nuclear Security Administration under contract DE-AC04-94AL85000. The views expressed herein are those of the authors and should not

be interpreted as necessarily representing the official policies or endorsements, either expressed or implied, of Sandia or the U.S. Government.

References

[1]Treanor, C. E. and Marrone, P. V., "Effect of Dissociation on the Rate of Vibrational Relaxation," *Physics of Fluids*, Vol. 5, No. 9, 1962, pp. 1022–1026.

[2]Chernyi, S. G., Losev, S. A., Macheret, S. O., and Potapkin, B. V., *Physical and Chemical Processes in Gas Dynamics: Cross Sections and Rate Constants Volume I*, Vol. 196, 2002.

[3]Bird, G. A., "A Comparison of Collision Energy-based and Temperature-based Procedures in Q-K," *Rarefied Gas Dynamics: Proceedings of the 26th International Symposium on Rarefied Gas Dynamics*, Vol. 1084, American Institute of Physics, Melville, NY, 2009.

[4]Bird, G. A., *Molecular Gas Dynamics and the Direct Simulation of Gas Flows*, Oxford University Press, 1994.

[5]Gallis, M. A., Bond, R. B., and Torczynski, J. R., "A Kinetic-Theory Approach for Computing Chemical-Reaction Rates in Upper-Atmosphere Hypersonic Flows," *Journal of Chemical Physics*, Vol. 131, No. 124311, 2009.

[6]Gallis, M. A., Bond, R. B., and Torczynski, J. R., "Assessment of Collisional-Energy-Based Models for Atmospheric Species Reactions in Hypersonic Flows," *Journal of Thermophysics and Heat Transfer*, Vol. 24, No. 2, April-June 2010.

[7]Gallis, M. A., Bond, R. B., and Torczynski, J. R., "Molecule-Based Approach for Computing Chemical-Reaction Rates in Upper Atmosphere Hypersonic Flows," SAND Report 2009-5286, Sandia National Laboratories, 2009.

[8]Bird, G. A., "The Q-K Model for Gas-Phase Chemical Reaction Rates," *Phys. Fluids*, Vol. 23, No. 106101, 2011.

[9]Nompelis, I., Drayna, T., and G.V.Candler, "Development of a Hypbrid Unstructured Implicit Solver for the Simulation of Reacting Flow Over Complex Geometries," Paper 2004-2227, AIAA, June 2004.

[10]Wright, M. J., Candler, G. V., and Bose, D., "A Data-Parallel Line-Relaxation Method for the Navier-Stokes Equations," Paper 97-2046, AIAA, June 1997.

[11]Millikan, R. C. and White, D. R., "Systematics of Vibrational Relaxation," *Journal of Chemical Physics*, Vol. 39, No. 12, 1963, pp. 3209–3213.

[12]Bose, D. and Candler, G. V., "Advanced Model of Nitric Oxide Formation in Hypersonic Flows," *Journal of Thermophysics and Heat Transfer*, Vol. 12, No. 2, April-June 1998, pp. 214–222.

[13]Bose, D., *Advanced Nitric Oxide Formation Modeling in Hypersonic Flows*, Ph.D. thesis, University of Minnesota, 1997.

[14]Boyd, I. D., Phillips, W. D., and Levin, D. A., "Prediction of Ultraviolet Radiation in Nonequilibrium Hypersonic Bow-Shock Waves," *Journal of Thermophysics and Heat Transfer*, Vol. 12, No. 1, 1998, pp. 38–44.

[15]Candler, G., Boyd, I., Levin, D., Moreau, S., and Erdman, P., "Continuum and DSMC Analysis of Bow Shock Flight Experiments," Paper 93-0275, AIAA, January 1993.

[16]Park, C., *Nonequilibrium Hypersonic Aerodynamics*, Wiley, 1990.

[17]Park, C., Howe, J. T., Jaffe, R. J., and Candler, G. V., "Review of Chemical-Kinetic Problems of Future NASA Missions, II: Mars Entries," *Journal of Thermophysics and Heat Transfer*, Vol. 8, No. 1, 1994, pp. 9–23.

[18]Bartel, T. J., Plimption, S. J., and Gallis, M. A., "Icarus: A 2-D Direct Simulation Monte Carlo (DSMC) Code for Multi-Processor Computers," SAND Report 2001-2901, Sandia National Laboratories, 2001.

[19]Erdman, P. W., Zipf, E. C., Espy, P., Howlett, C., Levin, D. A., Loda, R., Collins, R. J., and Candler, G. V., "Flight Measurements of Low-Velocity Bow Shock Ultraviolet Radiation," *Journal of Thermophysics and Heat Transfer*, Vol. 7, No. 1, Jan.-March 1993, pp. 37–41.

[20]Erdman, P. W., Zipf, E. C., Espy, P., Howlett, L. C., Levin, D. A., Collins, R. J., and Candler, G. V., "Measurements of Ultraviolet Radiation from a 5-km/s Bow Shock," *Journal of Thermophysics and Heat Transfer*, Vol. 8, No. 3, July-Sept. 1994, pp. 441–446.

[21]Boyd, I. D., Bose, D., and Candler, G. V., "Monte Carlo Modeling of Nitric Oxide Formation Based on Quasi-Classical Trajectory Calculations," *Phys. Fluids*, Vol. 9, 1997, pp. 1162.

[22]Levin, D. A., Candler, G. V., Collins, R. J., Erdman, P. W., Zipf, E., and Howlett, C., "Examination of Theory for Bow Shock Ultraviolet Rocket Experiments - I," *Journal of Thermophysics and Heat Transfer*, Vol. 8, No. 3, July-Sept. 1994, pp. 447–452.

[23]Levin, D. A., Braunstein, M., Candler, G. V., Collins, R. J., and Smith, G. P., "Examination of Theory for Bow Shock Ultraviolet Rocket Experiments - II," *Journal of Thermophysics and Heat Transfer*, Vol. 8, No. 3, July-Sept. 1994, pp. 453–459.

[24]Levin, D. A., Candler, G. V., Collins, R. J., Erdman, P. W., Zipf, E. C., and Howlett, C. L., "Examination of Ultraviolet Radiation Theory for Bow Shock Rocket Experiments," Paper 92-2871, AIAA, 1992.

VIII. Appendix

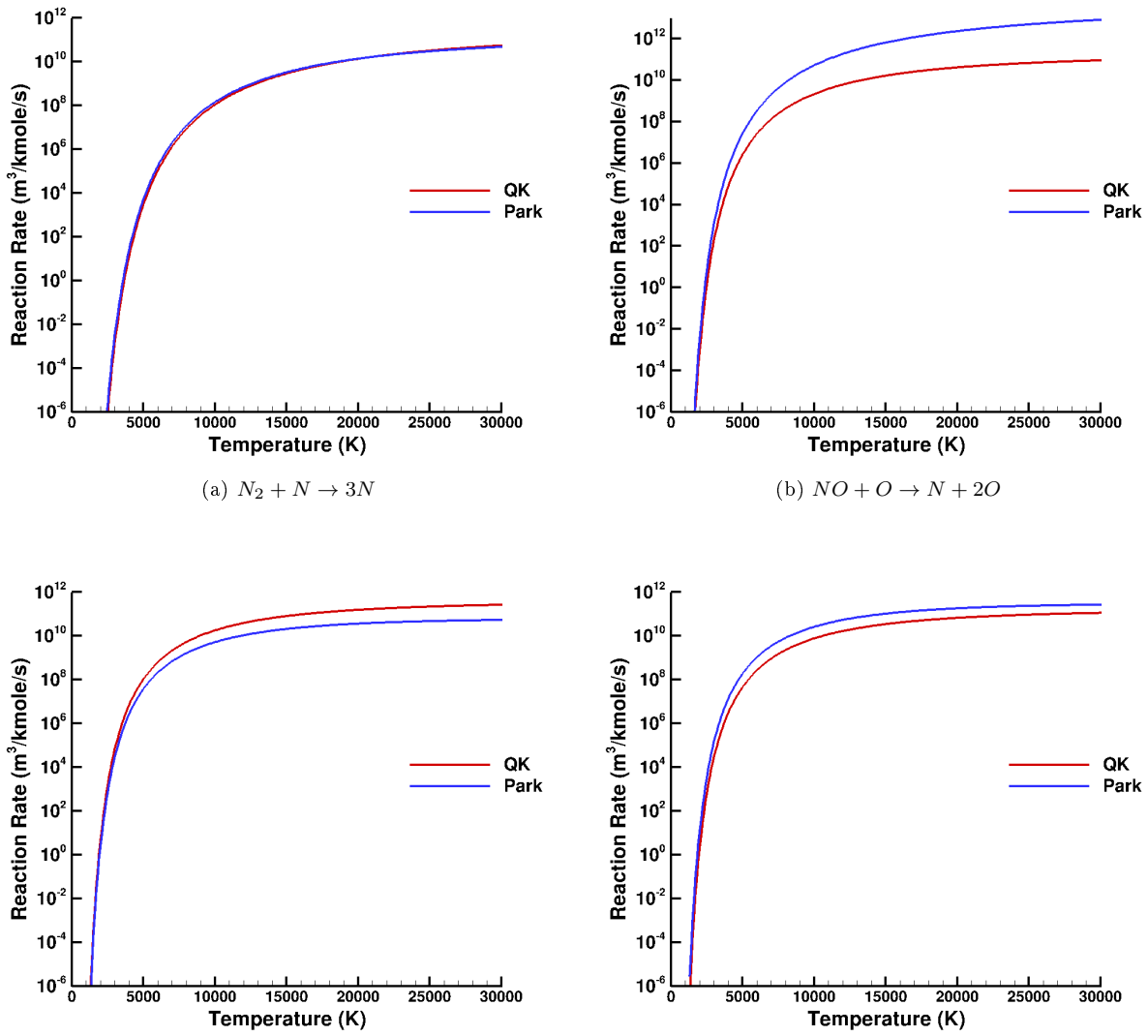

(a) $N_2 + N \rightarrow 3N$

(b) $NO + O \rightarrow N + 2O$

(c) $O_2 + O_2 \rightarrow 2O + O_2$

(d) $O_2 + O \rightarrow 3O$

Figure 11: Comparisons of dissociation reaction rates between the Park and Q-K models in thermal equilibrium.

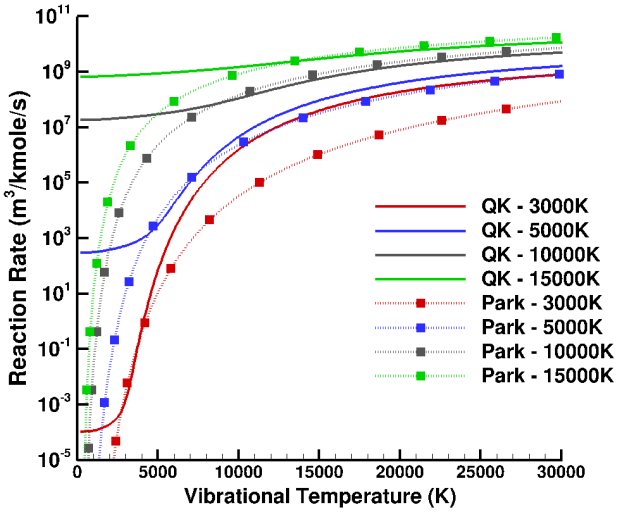

(a) $N_2 + N \rightarrow 3N$

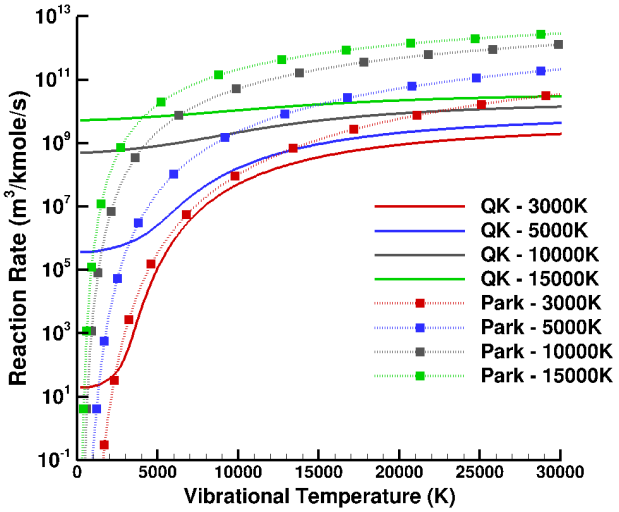

(b) $NO + O \rightarrow N + 2O$

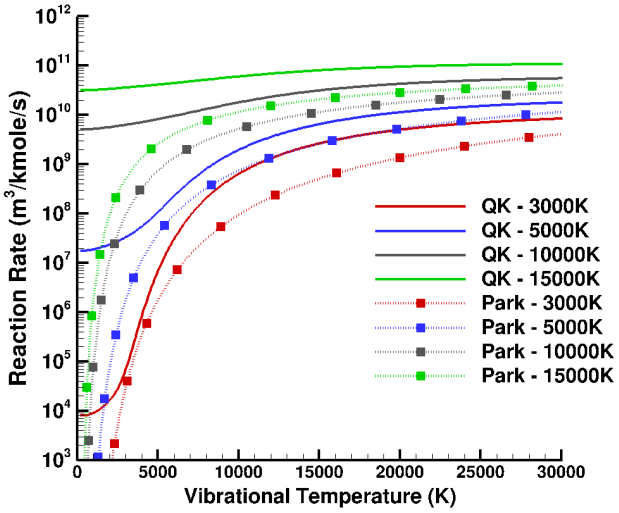

(c) $O_2 + O_2 \rightarrow 2O + O_2$

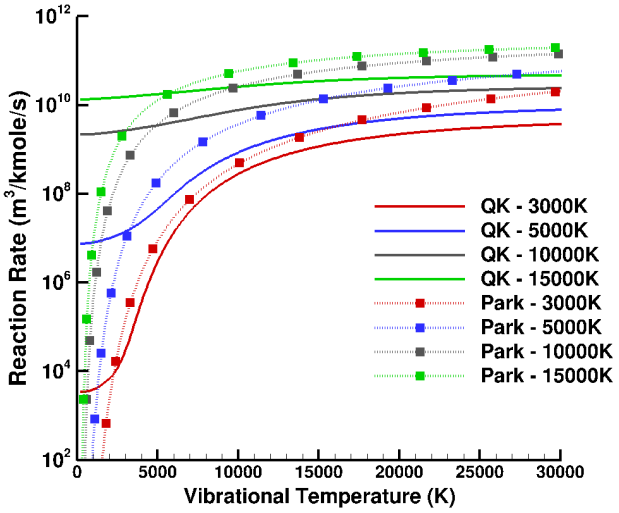

(d) $O_2 + O \rightarrow 3O$

Figure 12: Comparisons of dissociation reaction rates between the Park and Q-K models in thermal non-equilibrium.